STUDY OF SOURCE, MAGNITUDE, AND RECURRENCE TIME OF LARGE EARTHQUAKES AFFECTING NORTHERN PUERTO RICO:
Collaborative Research, M. Tuttle & Associates and Central Region Hazards Team, U.S. Geological Survey

Final Technical Report

Research supported by the U.S. Geological Survey (USGS),
Department of the Interior, under USGS award 1434-06HQGR0023

Martitia P. Tuttle
M. Tuttle & Associates
128 Tibbetts Lane
Georgetown, ME 04548
Tel: 207-371-2007
E-mail: mptuttle@earthlink.net
URL: http://www.mptuttle.com

Project Period: 2/1/2006-5/30/2007

Program Element II: Research on Earthquake Occurrence and Effects
Program Element I: Products for Earthquake Loss Reduction

Key Words: Paleoseismology, Paleoliquefaction, Age Dating, Quaternary Fault Behavior

STUDY OF SOURCE, MAGNITUDE, AND RECURRENCE TIME OF LARGE EARTHQUAKES AFFECTING NORTHERN PUERTO RICO: Collaborative Research, M. Tuttle & Associates and Central Region Hazards Team, U.S. Geological Survey

Martitia P. Tuttle
M. Tuttle & Associates
128 Tibbetts Lane
Georgetown, ME 04548
Tel: 207-371-2007
E-mail: mptuttle@earthlink.net

Abstract

During a previous paleoliquefaction study, we discovered dozens of liquefaction features in western Puerto Rico that probably formed during at least three large earthquakes since A.D. 1300, including the A.D. 1918 moment magnitude, **M**, ~7.5, event, the A.D. 1670 event, which may have been as large as **M** 7, and an earlier **M** ≥ 6.5 earthquake between A.D. 1300 and 1508. During this study, we resurveyed about 13 km of the Río Culebrinas in northwestern Puerto Rico and found an additional fourteen liquefaction features that are consistent with the earlier results. We also searched about 86 km of rivers in northern and eastern Puerto Rico and found fifteen liquefaction features, all along the Río Grande de Manati and Río de la Plata, on the north-central coast. Along the Río Grande de Manati, we found three generations of liquefaction features that probably formed during the A.D. 1943 **M** ~7.7 and A.D. 1787 **M** ~8.0 earthquakes and an earlier event between 1190-400 B.C. or about 800 B.C. ± 400 years. Along the Río de la Plata, small weathered sand dikes may have formed during the A.D. 1787 event. The features on the Río Manati that formed during the circa 800 B.C. event, including a 22 cm thick sand blow and 40 cm wide sand dike, are very weathered, larger than the historical features, and associated with vertical ground displacement and graben formation. The relatively large size of liquefaction features and severity of ground failure suggest that ground shaking was stronger along the north-central coast during the 800 B.C. earthquake than during the A.D. 1943 and A.D. 1787 earthquakes. This implies that the 800 B.C. earthquake was either larger than the historical earthquakes or located closer to the north-central coast of Puerto Rico. Also, the paleoliquefaction data suggest that the 800 B.C.-type earthquake has a recurrence time of more than 2,800 years, considerably longer than that estimated for **M** ~8 earthquakes generated by the Puerto Rico subduction zone. The lack of liquefaction features along rivers in northeastern and eastern Puerto Rico, especially along Rio Blanco where sedimentary conditions are suitable for the formation of liquefaction features, suggest that this area may not have been subjected to strong shaking during the past 2,000 years.

Introduction

Puerto Rico is located within a diffuse and complex boundary zone between the North American and Caribbean tectonic plates (Figure 1). The North American plate is moving west-southwest relative to the Caribbean plate at a rate of 19.4 mm/yr (Jansma et al., 2000; Lopez, 2006). Motion along the northern portion of the plate boundary is left-lateral strike-slip, with varying amounts of transpression and transtension (e.g., Sykes et al., 1982; Mann et al., 1990; Deng and Sykes, 1995; Mann et al., 2002). Puerto Rico and the Virgin Islands (PRVI) appear to comprise a microplate that is bounded by the Puerto Rico Trench to the north, the Muertos Trough to the

south, the Anegada Passage to the east and southeast, and the Mona Passage to the west (Figure 1; e.g., Masson and Scanlon, 1991; Dixon et al., 1998; Lopez et al., 1999). Side-scan sonar imagery, single-channel seismic data, and GPS geodetic measurements indicate extensive normal faulting of the carbonate platform in the central and western portion of the Mona Passage, reflecting differential eastward relative motion of the PRVI and Hispaniola microplates (e.g., Van Gestel et al., 1998; Lopez et al., 1999; Jansma et al., 2000).

Puerto Rico, home to about 3.9 million U.S. citizens with about 2.7 million living in San Juan on the north coast, is densely settled with most of the population and urban development concentrated in coastal areas. As demonstrated by the record of historical earthquakes, these coastal areas are subject to tsunami inundation and liquefaction as well as strong ground shaking. Historical earthquakes include a moment magnitude, **M** ~7.7 event in 1943 located northwest of Puerto Rico, a **M** ~7.5 event in 1918 centered in the Mona Passage, a **M** ~7.3 event in 1867 in the Anegada Passage, a **M** ~8.0 event in 1787 possibly related to rupture of the Puerto Rico subduction zone, and a **M** ~6 event in 1670 in western Puerto Rico (e.g., Reid and Taber, 1919; McCann, 1985; Mueller et al., 2003; Prentice and Mann, 2005; see Figure 1). The 1867 earthquake produced a tsunami that was especially damaging to the U.S. Virgin Islands and struck southeastern Puerto Rico with 1 to 6 m high waves (Landers et al., 2002). The 1918 earthquake and related tsunami had their greatest impact on the western coast of Puerto Rico, killing at least 114 persons and causing 4 million dollars in damage (Reid and Taber, 1919). This earthquake also induced liquefaction in the Río Anasco valley and near Aguadilla (Figure 2; Moya and McCann, 1991). The **M** 8.1 1946 earthquake in northeastern Dominican Republic also triggered a tsunami that killed ~1700 people in the northern Caribbean and washed ashore in Aguadilla and was recorded at San Juan (Landers et al., 2002; Grindlay et al., 2005).

Most earthquake sources significant to Puerto Rico are thought to be located offshore. These sources include the Puerto Rico subduction zone extending southward from the Puerto Rico trench, North Puerto Rico Slope fault zone (NPRSFZ), South Puerto Rico Slope fault zone (SPRSFZ), Septentrional fault zone (SFZ), and faults associated with the Mona Passage, Virgin Islands Trough, and Los Muertos Trough (Figure 1). Major onshore fault zones include the Great Southern Puerto Rico fault zone (GSPRFZ) and the Great Northern Puerto Rico fault zone (GNPRFZ) (Figure 2). The GNPRFZ is a major northwest to west-northwest trending, left-lateral strike-slip fault system that crosses the northern part of the island about 20 km south of San Juan, with one or more splays approaching the suburbs of the city. The fault zone offsets lower Cretaceous to Eocene rocks and is overlain by middle Tertiary strata along the north coast (e.g., Monroe, 1980). Although small shallow earthquakes are spatially associated with the structure (McCann, 1985), the fault zone is thought to be inactive at least during the Holocene (Geomatrix, 1988; Williams and Tuttle, 2010).

The GSPRFZ is another major northwest-trending, left-lateral strike-slip fault system that crosses southern and western Puerto Rico. It is also characterized by dip-slip displacement in the south-central part of the island (Geomatrix, 1988). Field investigations of the GSPRFZ by the Department of Geology at the University of Puerto Rico documented two phases of normal faulting, one phase during the Oligocene and the other after the Oligocene. In the 1970s, trenching of faults in the system uncovered evidence of Quaternary faulting in the south (Geomatrix, 1988). More recently, single- and multi-channel seismic data collected across the offshore extension of the Cerro Godin fault, a member of the GSPRFZ located ~10 km north of

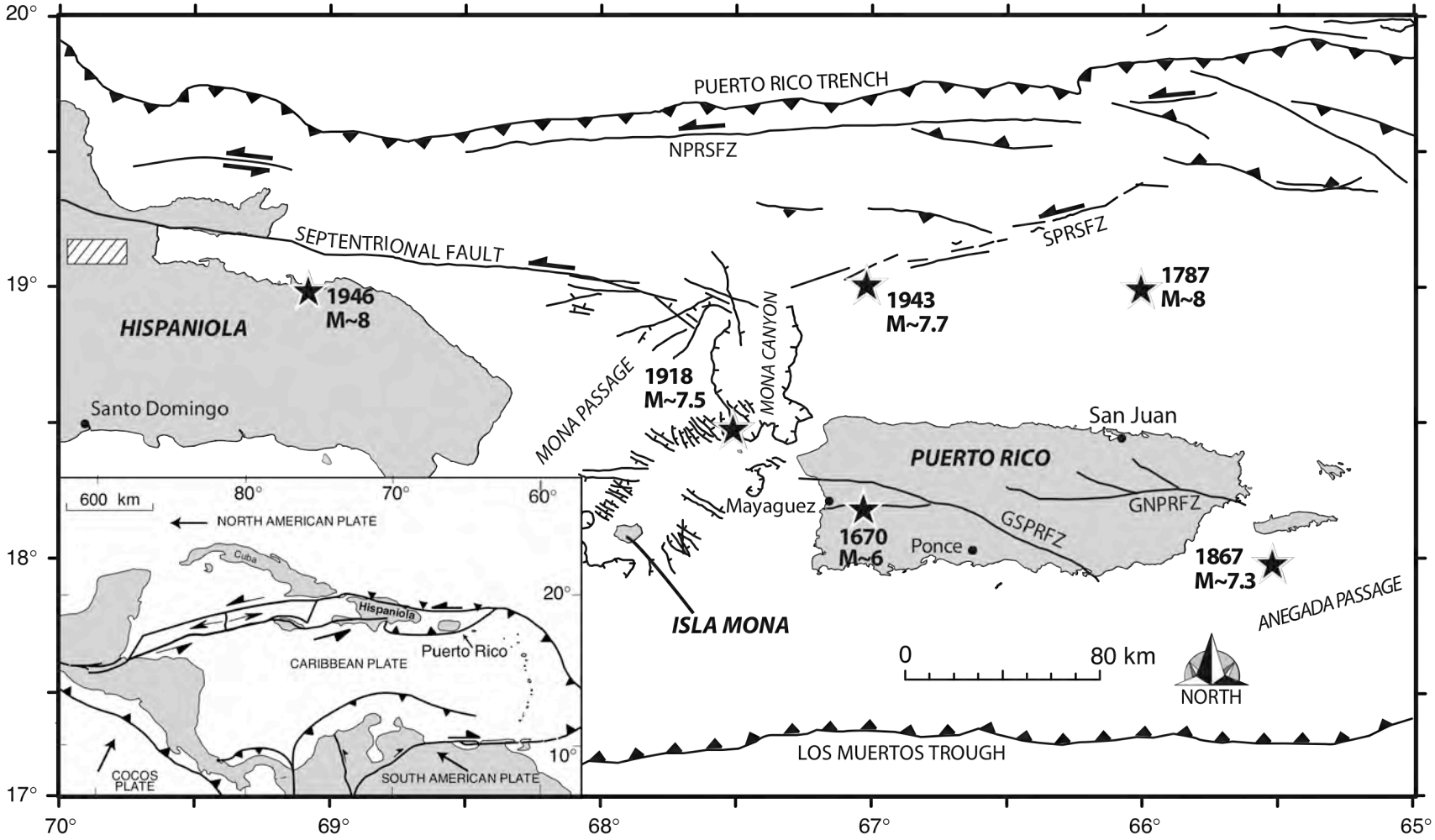

Figure 1. Northeastern Caribbean showing Puerto Rico and locations of large historical earthquakes and major onshore and offshore faults (1986 MIDAS catalog; McCann, 1985; Grindlay et al., 1997; Dolan et al., 1998; Mueller et al., 2003). GNPRFZ = Great Northern Puerto Rico fault zone; GSPRFZ = Great Southern Puerto Rico fault zone; NPRSFZ = Northern Puerto Rico Slope fault zone; SPRSFZ = Southern Puerto Rico Slope fault zone. Liquefaction features found on Hispaniola related to **M** ~8 earthquakes in 1946 and possibly in A.D. 1200, indicated by rectangle (Tuttle et al., 2003). Inset map shows tectonic setting of Caribbean region.

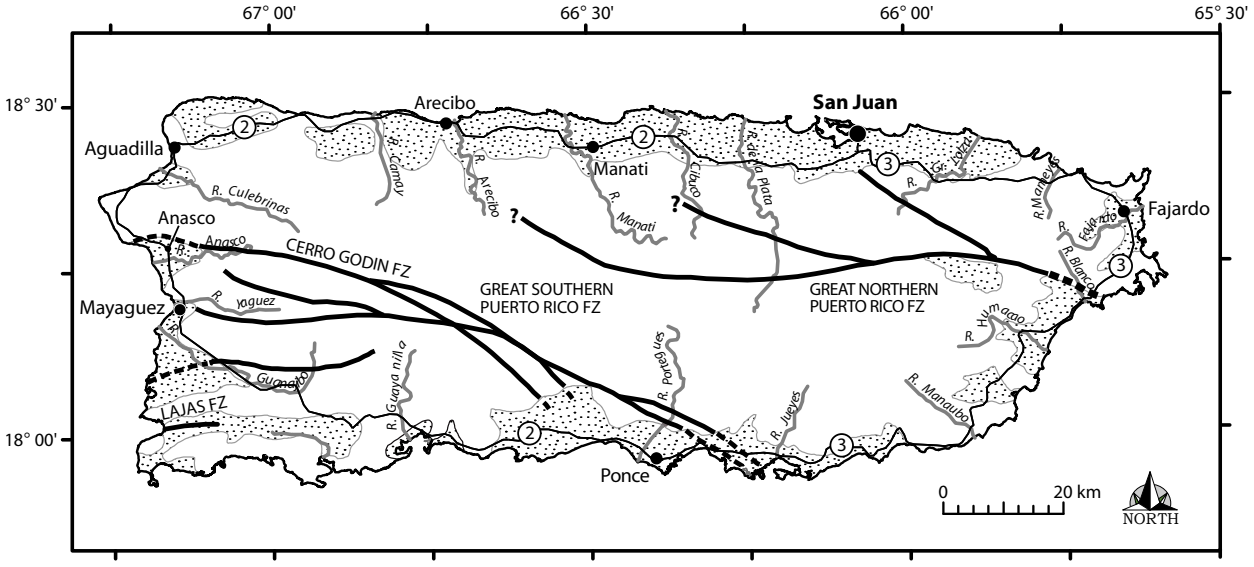

Figure 2. Map of Puerto Rico showing rivers, Quaternary sediments (stippled pattern), and major onshore faults (heavy black lines) (e.g., Briggs, 1964; Geomatrix, 1988; Prentice and Mann, 2005).

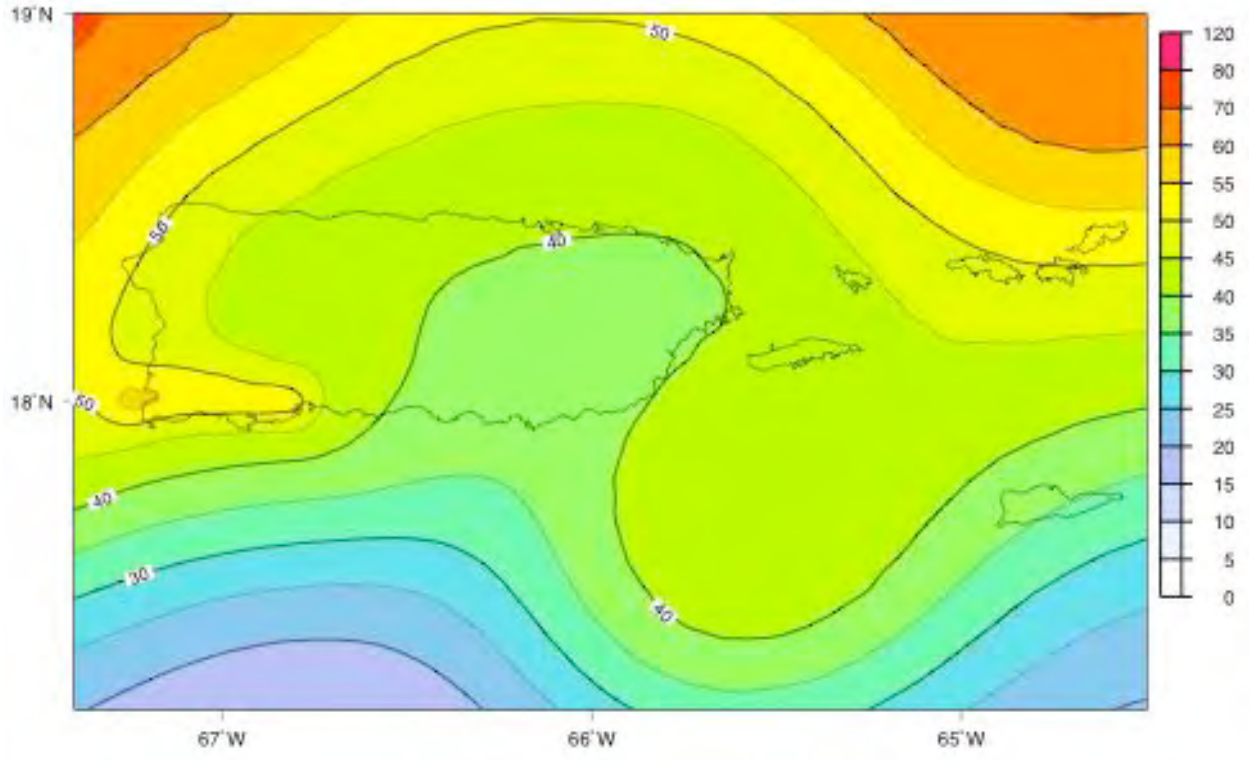

Figure 3. Hazard map of peak ground acceleration (% g) with 2% probability of exceedence in 50 years from all modeled source (from Mueller et al., 2003). Note influence of Lajas fault in southwestern Puerto Rico on hazard map.

Mayaguez, suggest fault displacements of Pliocene and possibly Holocene sediment (Prentice et al., 2003a). Although geomorphic features suggest possible late Quaternary right-lateral displacement, no unequivocal evidence of faulting has been found in excavations across projected surface traces of the inferred faults (Mann et al., 2005; C. Prentice, pers. comm., 2011).

In southwestern Puerto Rico, an area of shallow seismicity (Asencio, 1980; McCann, 1985), the South Lajas fault was found to have ruptured the surface twice in the past 7,500 years (Prentice et al., 2000; Prentice and Mann, 2005). Based on an estimated total fault length of 50 km, these earthquakes may have been of **M** 7.0 (LaForge and McCann, 2005). This finding strongly influences the seismic hazard map for the southwestern part of the island (see Figure 3).

The research reported below was conducted in collaboration with Eugene Schweig of the U.S. Geological Survey. Dori Bellan, Kathleen Dyer-Williams, Sarah Kroupa, Juan Carlos Moya, Rafael Prieto, John Sims, and Holly Schroeder assisted with reconnaissance. Dyer-Williams also compiled and analyzed geotechnical data and Kathy Tucker assisted with mapping. Beta Analytic Radiocarbon Laboratory performed radiocarbon dating for this project.

Search for Earthquake-Induced Liquefaction Features

During this project, we searched for earthquake-induced liquefaction features along 99 km of river length including the Río Culebrinas along the northwest coast, Río Grande de Arecibo, Río Grande de Manati, Río Cibuco, Río de La Plata, Río Canovanas, Río Espiritu Santo, and Río Mameyes along the northern coast, and Río Fajardo, Río Blanco, and Río Maunabo along the eastern coast (Figure 2; Table 1). It is preferable to survey 10-15 km of river length to evaluate the presence or absence of liquefaction features. Several of the rivers along the northern and eastern coasts only had short sections along which Holocene deposits were exposed. For this reason, we surveyed many rivers in order to evaluate more exposure and to get a broader regional view. We did not search rivers along the southern coast because there were even fewer exposures of Holocene deposits. We found and documented earthquake-induced liquefaction features, including two sand blows and twenty-eight sand dikes, at fourteen liquefaction sites and collected organic samples at many of those sites for radiocarbon dating (Tables 2 and 3). Beta Analytic Radiocarbon Laboratory performed dating of selected samples from twelve sites (Table 4). The results of radiocarbon dating and the degree of weathering of sand blows and sand dikes were used to estimate the ages of the features. In general, we assumed that liquefaction features that formed during the historical period probably formed as the result of known large historical earthquakes.

<u>Río Culebrinas</u>

During a previous project, we found twenty-seven liquefaction features at ten sites along the Río Culebrinas. These features include sand dikes up to 23 cm wide and one, possibly two, sand blow deposits (Tuttle et al., 2005). Many of the features probably formed during the A.D. 1918 or A.D. 1670 earthquakes; but at least one of the sand blows and related sand dikes formed between A.D. 1300 and 1508, suggesting that a large earthquake caused strong ground shaking in northwestern Puerto Rico during that time.

For this study, we resurveyed 13.3 km of the Río Culebrinas from upstream of the Rt. 110 to the coast hoping to find additional features that might help to constrain the source area and magnitude of the A.D. 1300-1508 earthquake (Figure 4). Along the upstream third of the river,

Table 1. Search for Earthquake-Induced Liquefaction Features in Puerto Rico.

River	River Section Searched	Section Length (km)	Suitable Conditions	River Bank Exposure	Liquefaction Features
Culebrinas	From upstream of the Rt. 110 to coast	13.3	Yes	Good to excellent in many river bends along upper and lower thirds of river	Yes
Grande de Arecibo	From bridge about 5 km upstream from Bajadero to coast	16.7	Not ideal	Good to excellent in river bends; occasional exposures along straight sections; otherwise vegetated	No
Grande de Manati	From dairy farm southwest of Manati to coast	22	Yes	Excellent exposure in frequent river bends; poor along lower 2 km	Yes
Cibuco	From Rt. 160 bridge to 0.6 km south of coast	8	Probably	Fair in most bends along upper half of river; otherwise vegetated	No
de La Plata	From Hwy 2 to coast	7	Yes	Good to excellent along upper two thirds of river; much poorer downstream	Yes
Canovanas	From Hwy 3 to confluence with Rio Loiza	3.7	Yes	Good to excellent in most river bends	No
Espiritu Santo	From Hwy 3 to police station about 1.7 km south of coast	3.2	Yes	Good in bends along upper third; otherwise poor	No
Mameyes	From access point on Rt. 191 south of Highway 3 to the coast	4.5	No	Good in bends along upper half; otherwise poor	No
Fajardo	From farm road SE of airport to 1.6 km west of coast	5.7	No	Good to excellent in upstream bends; not as good downstream	No
Blanco	From Rt. 31 bridge in Rio Blanco to coast	10	Yes	Good to excellent in upstream bends; poorer downstream	No
Maunabo	From farm road 2 km west of Maunabo to coast	4.7	Possibly	Good in bends along upstream section; poor downstream	No

Figure 4. Google Earth image showing portion of Río Culebrinas surveyed (red lines) totaling 13.3 km. Site locations indicated by white dots.

most cutbanks were 5-8 m high and exposure was good to excellent in river bends. Typically, cutbanks exposed reddish silt and sandy silt in which 2-7 paleosols had formed.

Along the middle third of the river, upstream from a dam and pumping station, the banks were mostly vegetated and there were few exposures. Along the downstream third of the river, cutbanks were 3-4 m high and there were excellent exposures in river bends. Cutbanks were composed primarily of reddish silt, with few interbeds of sand, in which multiple paleosols had formed. At several locations, sand and pebbley sand was observed at the base of the cutbank or detected with a soil probe up to 0.9 m below the cutbank. Along the lowermost 1 km, the banks were low and vegetated.

Sediments along the Río Culebrinas are interpreted as Holocene fluvial deposits of sandy clay and clayey sand (Monroe, 1969). Sedimentary conditions in the floodplain of silt overlying sand are suitable for the formation of earthquake-induced liquefaction features. Borehole data

collected near the Highway 2 crossing of the river indicate that moderately dense sand occurs below the surface. Liquefaction potential analysis found that a local earthquake (5 km distance) would have to be of **M** 6.5 to induce liquefaction in at this site (Tuttle et al., 2005).
During this study, we found an additional fourteen liquefaction features including, one sand blow and thirteen sand dikes at seven sites (Table 2). These findings on the Río Culebrinas are consistent with our earlier findings and suggest that earthquakes induced liquefaction in this area at least three times during the past 700 years, during the A.D. 1918 and A.D. 1670 earthquakes and during an earlier event between A.D. 1300 and 1508.

Table 2. Liquefaction Sites along the Northwestern Coast of Puerto Rico.

Site Name	Latitude (Decimal Degrees)	Longitude (Decimal Degrees)	Thickness of Sand Blows (cm)	Width of Sand Dikes (cm)	Strike and Dip of Largest Sand Dikes	Preliminary Age Estimate of Features
Río Culebrinas						
RC 11	18.39923	67.15766		18, 12, 6, 3	N87°W, 86°SW N24°E, 85°NW	Since A.D. 1530; probably A.D. 1670 event
RC 12	18.39938	67.15775		7, 4, 2.5	Similar to 11	Since A.D. 1530; probably A.D. 1670 event
RC 13	18.40017	67.16224	12	8, 1	N48°E, 80°NW N72°W, 76°NE	Since A.D. 1670; probably A.D. 1918 event
RC 100	18.37604	67.11758		8	N37°E, 80°SE	Possibly A.D. 1300-1508 and A.D. 1670 events
RC 101	18.38203	67.12594		12	N22°W, 88°SW	Since A.D. 1160; possibly A.D. 1300-1508 and A.D. 1670 events
RC 102	18.38832	67.13261		3	N42°W, 84°SW	Possibly A.D. 1300-1508 and A.D. 1670 events
RC 103	18.39019	67.14146		2	N19°W, 74°NE	Possibly A.D. 1300-1508 and A.D. 1670 events

At sites RC 11 and nearby site RC 12, we documented seven sand dikes, the largest one being 18 cm wide. A sample of charred material collected 3 cm below the tip of one of the dikes at RC 11 yielded a calibrated date of A.D. 1530-1560, 1630-1680, 1740-1800, and 1930-1950, suggesting that the dikes formed since A.D. 1530 (Table 4). In addition, the sand dikes at the two sites were iron-stained and exhibited accumulated fines, suggesting that they formed more than one hundred years ago, and therefore, probably during the A.D. 1670 earthquake.

At site RC 13, we documented a 12 cm thick sand blow and two sand dikes. A sample of charred material collected 12 cm below sand blow yielded a calibrated date of A.D. 1670-1770,

1800-1940, and 1950, suggesting that the dikes formed since A.D. 1670 (Table 4). A sample of charred material collected 22 cm above the sand blow gave a similar result. Some iron staining but no fines accumulation was noted for the dikes. Therefore, these dikes more likely formed during the A.D. 1918 earthquake than the A.D. 1670 event.

At site RC 100, we documented an 8 cm wide sand dike (Figure 5). The sand dike was composed of two phases of sand suggesting two episodes of formation. The sand in the dike was iron-stained. At site RC 101, we found a 12 cm wide dike that, like the dike at RC 100, was composed of two phases of sand and was iron-stained. A sample of charred material collected 20 cm below the tip of dike yielded a date of A.D. 1160-1270, suggesting that the dikes formed since A.D. 1160. Given the degree of weathering, the sand dikes probably formed more than one hundred years ago. Although not required, the two-phase dikes may have formed during two earthquakes, the A.D. 1300-1508 and A.D. 1670 events.

Figure 5. Sand dike at site RC 100 crosscuts reddish silts and mottled light brown paleosol near top of exposure. Iron staining of dike suggests it formed prior to the A.D. 1918 earthquake.

At sites RC 102 and RC 103, we documented a 3 cm wide dike and a 2 cm wide dike, respectively. Both dikes were iron-stained for most if not all of their exposed heights, suggesting

that they probably formed prior to the A.D. 1918 earthquake during either the A.D. 1300-1508 or A.D. 1670 events.

At site RC 104 about 1.3 km from the coast, we found an unusual sandy layer containing shells and lithic fragments that might be a tsunami deposit. Two samples of charred material collected from the possible tsunami sand layer and from a paleosol on which it was deposited yielded similar radiocarbon dates, A.D. 1660-1950, indicating that the layer was deposited since A.D. 1660. Tsunamis generated by the 1918 earthquake in Mona Canyon and the 1946 earthquake in northeastern Dominican Republic are known to have struck the northwestern coast, affecting communities near the mouth of Río Culebrinas.

Río Grande de Arecibo

Figure 6. Google Earth image showing portion of Río Grande de Arecibo surveyed (red line) totaling 16.7 km. Site locations indicated by white dots.

We surveyed 16.7 km of the Río Grande de Arecibo from a bridge crossing about 5 km upstream from Bajadero to the coast. Along the upstream half of the river, cutbanks were 3-6 m high and exposure was good to excellent in infrequent river bends. Exposed in the cutbanks, light brown silt with lenses of sand overlies sand, pebbles, and cobbles, and even boulders along the uppermost 2.5 km of the river. One to two paleosols had formed in the silt.

Along the downstream half of the river, cutbanks were 2-4 m high and exposure was good in more frequent river bends. Similar to the upstream section, light brown silt characterized by paleosols and lenses of sand overlies sand, pebbles, and cobbles. In a few locations, there were two fining upward sequences of sand and silt. In general, there was more sand and fewer boulders exposed along the downstream section, indicating that the deposits fine away from the mountains. However, pebbles and cobbles were commonly exposed at the base of the cutbank or detected with a soil probe within 0.5 m below the cutbank. Along the lowermost 0.5 km, the banks were low and vegetated.

Sediments along the Río Grande de Arecibo are interpreted as Holocene floodplain alluvium including sand, silt, and clay and coarse channel deposits (Briggs, 1968). We found no earthquake-induced liquefaction features along the river but this may be due to the high percentage of pebbles, cobbles, and boulders in the coarse fraction of the alluvium. These coarse materials would be exceedingly difficult to liquefy.

Río Grande de Manati

We surveyed 22 km of the Río Grande de Manati from a dairy farm about 3 km southwest of the town of Manati to the coast (Figure 7). Along the upstream third of the river close to the mountains, cutbanks were 5-7 m high and exposure was excellent in frequent river bends. Exposed in the cutbanks, reddish silt and interbedded sand overlie pebbles and cobbles. Multiple paleosols had formed in the silt. Along the middle third, cutbanks were 4-6 m high and exposure was excellent in frequent river bends. Reddish silt and clayey silt, in which as many as six paleosols had formed, were exposed in the cutbanks. At several locations silty sand and sand were exposed at the base of the cutbank or detected with a soil probe within 1 m below the cutbank. Along the lower third of the river, cutbanks were 1-4 m high and exposures became increasingly low and rare as the coast was approached. Along this section, reddish silt and clayey silt, in which two to four paleosols had formed, overlie silty sand and sand. As determined with a soil probe, sandy sediment often extended at least 1 m below the cutbank.

Sediments along the Río Grande de Manati are interpreted as Holocene alluvium including sand, silt, clay, and pebbles beneath the coastal plain (Briggs, 1965) and sand, silt, clay, and cobbles near the mountains (Monroe, 1971). Near the mountains, the high percentage of pebbles, cobbles in the coarse fraction of the alluvium reduced the liquefaction susceptibility of the sediments. However, beneath the coastal plain and away from the mountains, the sedimentary conditions are suitable for the formation of liquefaction features and to record strong ground shaking for the past 5,000 years. Borehole data collected along Highway 2 and along Rt. 140 near Barceloneta indicate that very loose to moderately dense sand occurs 3-10 m below the surface.

During this study, we found fourteen liquefaction features including, one sand blow and thirteen sand dikes at six sites (Table 3). These findings suggest that earthquakes induced liquefaction in

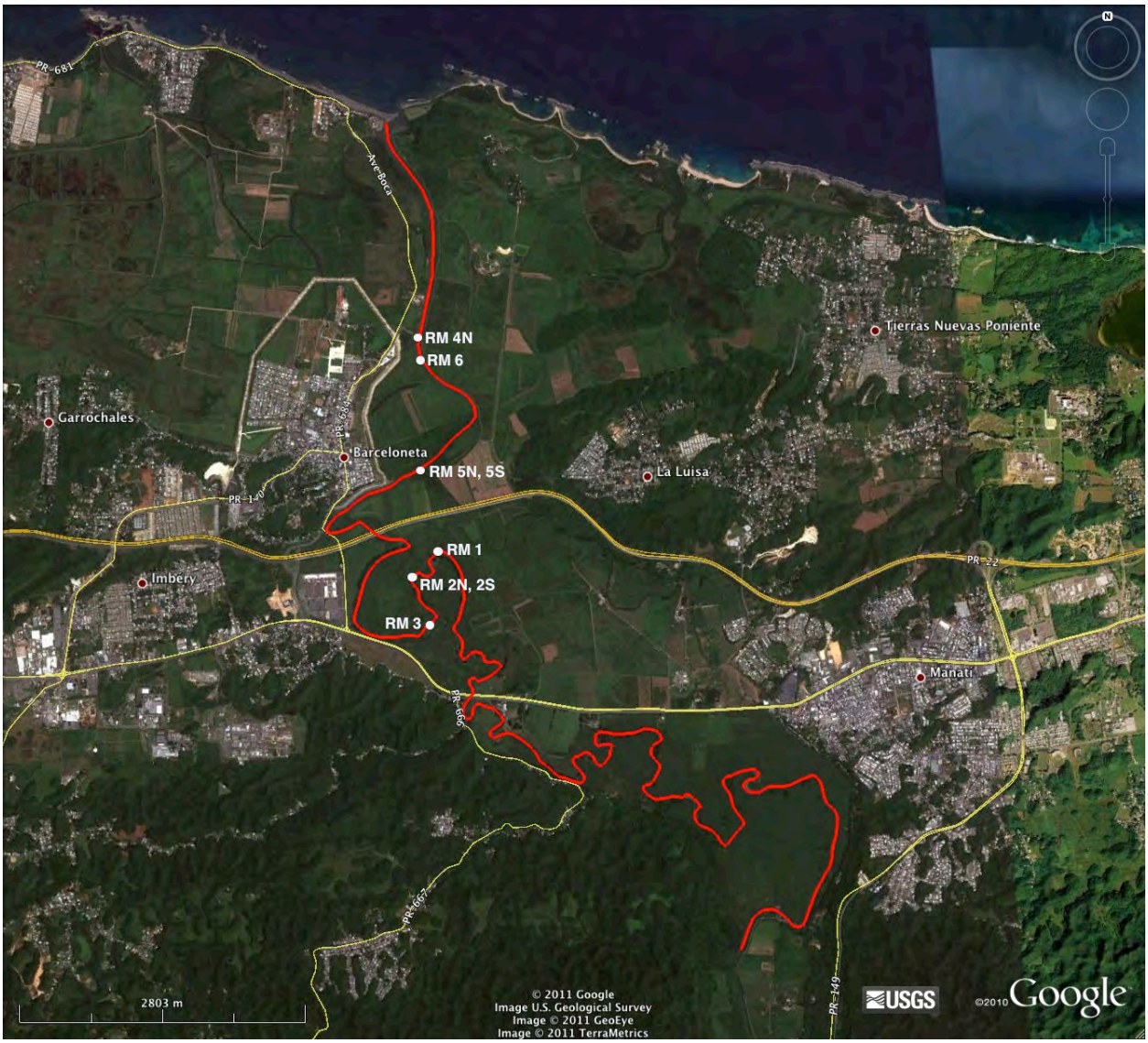

Figure 7. Google Earth image showing portion of Río Grande de Manati surveyed (red line) totaling 22 km. Site locations indicated by white dots.

this area at least three times during the past 5,000 years, during the A.D. 1943 and A.D. 1787 earthquakes and during an earlier event between 1190-400 B.C. The relatively large size of the older liquefaction features and severity of ground failure caused by the circa 800 B.C event suggest that it was larger than or located closer to the Manati river valley than the historical earthquakes.

At site RM 1, we documented a sand blow and four sand dikes (Table 3 and Figure 8). The 22 cm thick sand blow was about 4 m below the surface and immediately above the next to lowest of six paleosols exposed in the cutbank. The sand blow was connected to a 10-20 cm wide sand dike. A sample of organic sediment collected from the paleosol immediately below the sand blow yielded a calibrated date of 1190-930 B.C. and a sample of organic sediment collected from the base of the paleosol overlying the sand blow yielded a calibrated date of 780-400 B.C.

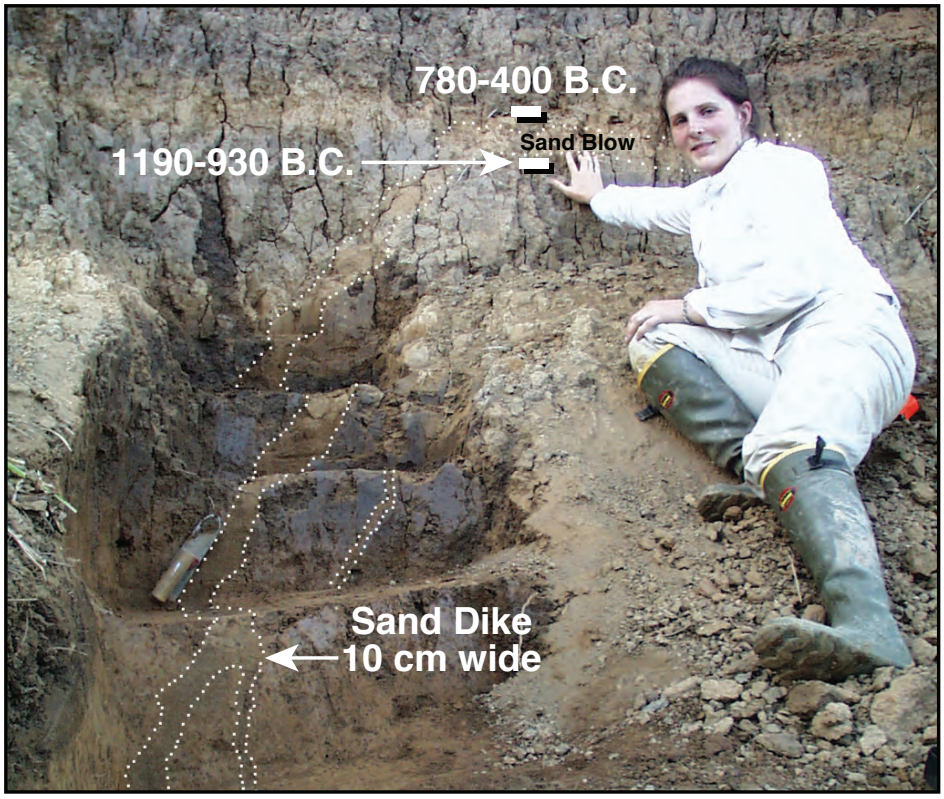

Figure 8. Photograph of earthquake-induced liquefaction features discovered at sites RM 1 (see Figure 7 for site location). Sand dike and related sand blow formed soon after 1190-930 B.C. and before 780-400 B.C. or about 800 B.C. ± 400 years.

(Table 4). These results suggest that the sand blow and related dike formed between 1190 and 400 B.C. (800 B.C. ± 400 years) but may be closer in age to 1190 B.C. than to 400 B.C. The sand blow had experienced soil development. It exhibited blocky structure and root pores. Sand grains were coated with fines and were stained by iron and manganese. The sand dikes also exhibited iron and manganese staining and fines accumulation. Also, the site appeared to have experienced a small amount of vertical displacement (8 cm) across the sand dike.

At site RM 2N, we documented a 40 cm wide sand dike and related overlying graben structure and three other small sand dikes (Table 3 and Figure 9). The large sand dike was iron-stained, mottled, and exhibited fines accumulation. The large dike and overlying graben probably formed at the same time and as a result of lateral spreading. During lateral spreading, a ground fissure probably formed into which water and entrained sand were injected from below and overlying silt and soil collapsed. Vertical displacement of paleosols across the large sand dike and related graben is about 5 cm. The uppermost paleosol disturbed by graben formation marks the approximate ground surface at the time of the event and provides maximum age constraint of 1430-1120 B.C. for the event. The overlying undisturbed paleosol provides a minimum age constraint of A.D. 230-540. Therefore, the features formed between 1430 B.C and A.D. 540. This age estimate has a broader range and overlaps that of the sand blow and related sand dike at nearby site RM 1. Therefore, all these features probably formed during the same event about 800 B.C. ± 400 years. Also at RM 2N, a 1.5 cm wide dike crosscut and clearly post-dated the larger dike. The small dike was also iron-stained and exhibited fine accumulation, suggesting that it did not form during the A.D. 1943 earthquake but possible during the A.D. 1787

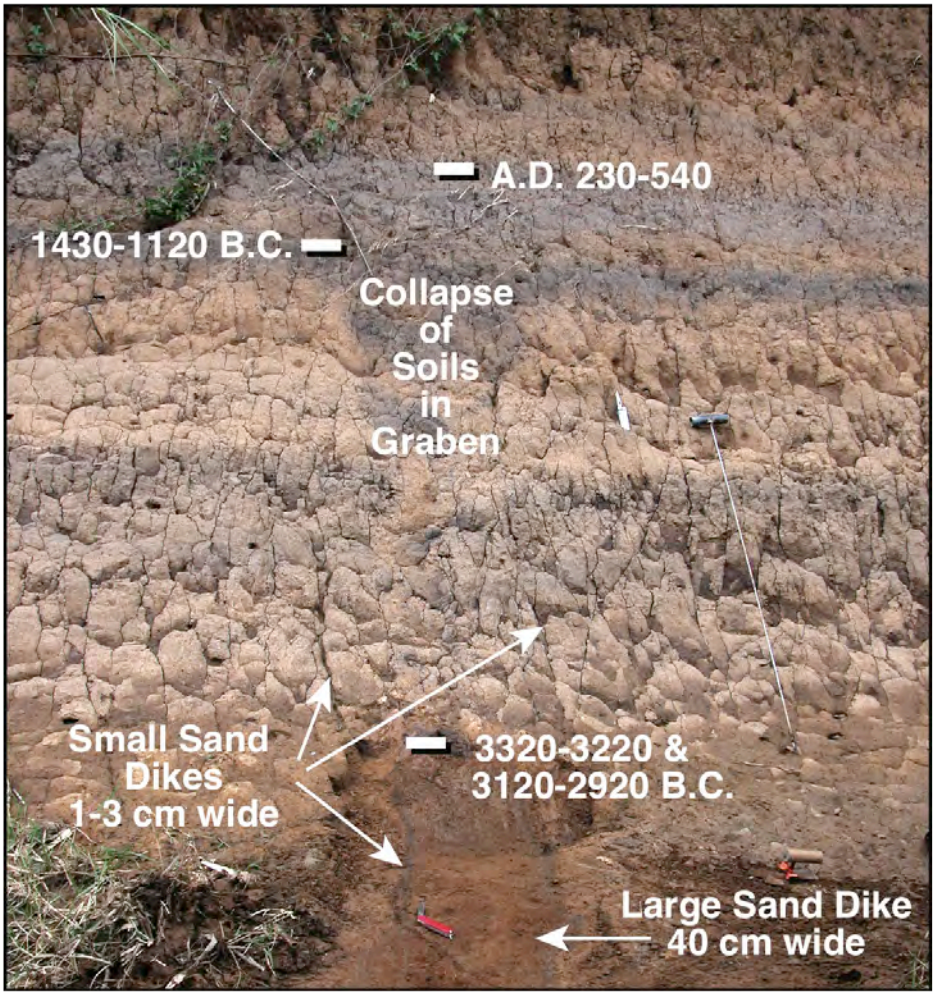

Figure 9. Photograph of liquefaction features discovered at sites RM 2N. Large very weathered sand dike (below) and collapse of overlying soils into graben (above) occurred soon after 1430-1120 B.C. and before A.D. 230-540, probably during same earthquake responsible for liquefaction features at nearby site RM 1. Large sand dike is crosscut by relatively small weathered dike. Two other small but unweathered dikes were intruded along the margins of large dike. For scale, soil probe on right is 1.5 m long.

earthquake. Two other small dikes, 3 and 2.5 cm wide, had intruded along the margins of the large dike. These dikes were essentially unweathered and may have formed during the A.D. 1943 earthquake.

At RM 2S, we found only one small, 1 cm wide, sand dike. The sand filling the dike was loose, exhibited no iron staining, or accumulation of fines. This feature was clearly young and probably formed during the A.D. 1943 event.

At RM 4N, we documented two sand dikes, 4 and 1.2 cm wide, that were iron stained and mottled. A sample of charred material collected 95 cm below the tip of the larger sand dike yielded a calibrated age of A.D. 1020-1220. Clearly, the dike formed after A.D. 1020. Given their degree of weathering, the dikes more likely formed during the A.D. 1787 event than the A.D. 1943 event.

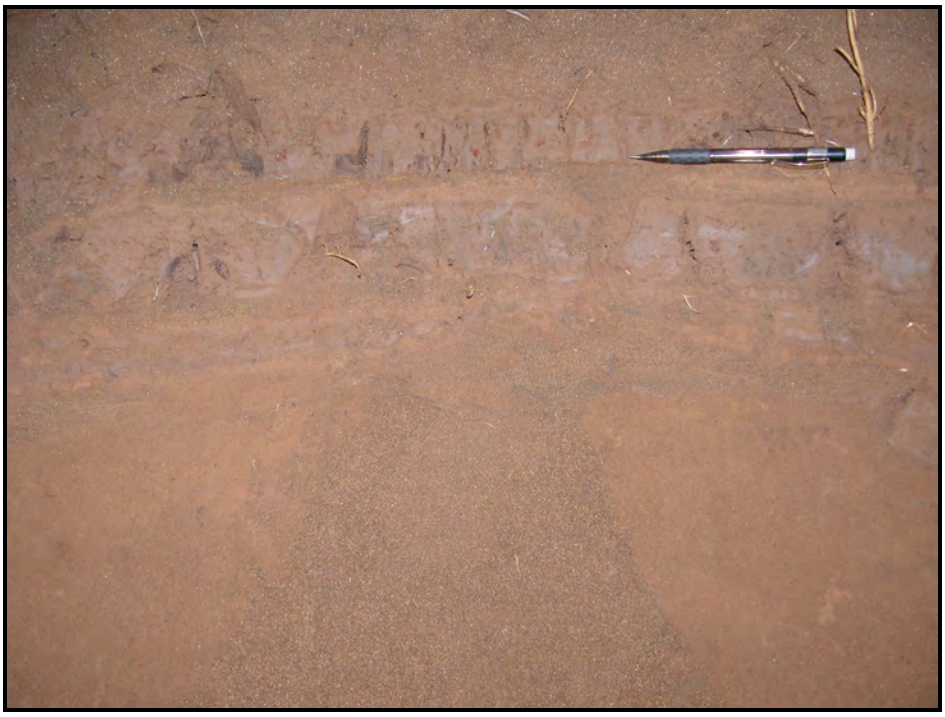

Figure 10. Sand dike at site RM 5N terminates as sills below layers of clayey silt about 2 m below the surface of the floodplain. Features appear redder in photograph than in reality.

Figure 11. At site RM 6, unusual fining upward deposit of pebbley shelly sand containing imbricated clasts of the underlying unit of cemented sandy silt as well as pieces of eolianite and brick. The imbricate arrangement of the clasts indicates that flow direction was upstream (towards the left).

Table 3. Liquefaction Sites along the North-Central Coast of Puerto Rico.

Site Name	Latitude (Decimal Degrees)	Longitude (Decimal Degrees)	Thickness of Sand Blows (cm)	Width of Sand Dikes (cm)	Strike and Dip of Largest Sand Dikes	Preliminary Age Estimate of Features
Río Grande de Manatí						
RM 1	18.44213	66.52921	22	34, 20, 0.5	N50°E, 55°NW N54°W, 81°SW	1190 - 400 B.C. event
RM 2N	18.44187	66.53231		40, 3, 2.5, 1.5	N57°W, 90° N80°E, 90°	Probably 1190 - 400 B.C. event; & possibly A.D. 1787 and A.D. 1943 events
RM 2S	18.44004	66.53176		1	N45°W, 84°NE	Probably A.D. 1943 event
RM 4N	18.46116	66.53184		4, 1.2	N40°E, 77°NW N23°E, vertical	Since A.D. 1020; possibly A.D. 1787 event
RM 5N	18.44825	66.53336		14-31	N40°W, 82°NE	Probably A.D. 1943 event
RM 5S	18.44753	66.53462		4	N5°W, 85°SW	Probably A.D. 1787 event
Río de la Plata						
RDLP 10	18.43264	66.25755		1.5, 0.5, 0.5	N10°E, 83°SE	Since A.D. 640; probably A.D. 1787 event

At site RM 5S, we found 4 cm wide dike of which the upper 15 cm exhibited iron staining and fines accumulation. This feature probably formed during the A.D. 1787 event.

At site RM 5N, a sand dike ranges from 14-31 cm wide and terminates as sills below layers of clayey silt. The sand filling the dike and sills is loose and only slightly iron stained. These features most likely formed during the A.D. 1943 event.

At site RM6 about 2 km from the coast, we found an unusual deposit that might be a tsunami deposit. It is a fining upward deposit of pebbley, shelly, sand containing imbricated clasts of the underlying unit of cemented sandy silt as well as pieces of eolinite and brick. The imbricate arrangement of the clasts indicates that the flow direction was upstream (towards the left). The upper part of the deposit was cemented and was overlain by a recent and uncemented sandy deposit. The deposit is likely fairly young and may have formed during the 1918 or 1946 tsunamis. The runup of the 1918 tsunami was reported to be 0.6 m at Arecibo and the 1946 tsunami was recorded at San Juan.

Río Cibuco

We surveyed 8 km of the Río Cibuco from the Rt. 160 crossing of the river to 0.6 km south of the coast (Figure 12). Along the upstream half of the river, cutbanks were 3-4 m high and

Figure 12. Google Earth image showing portion of Río Cibuco surveyed (red line) totaling 8 km. Exposure was fair along the upper half of the river and poor along the lower half. Overall, exposure was very limited.

exposure was fair in most river bends. Reddish brown silt containing up to three paleosols were exposed in the cutbanks. Occassionally, sand with few granules and pebbles was interbedded with the silt or detected with a soil probe about 1 m below the cutbanks. Along the channelized downstream half of the river, cutbank exposures were less frequent but exposed similar sediments. The banks along the lowermost 1.5 km were mostly vegetated.

Sediments along the Río Cibuco are interpreted as Holocene floodplain alluvium including sand, clay, silt, sand, and pebbles (Monroe, 1963). Swamp deposits occur along the lower part of the river. Sedimentary conditions are likely to be suitable for the formation of liquefaction features. However, no liquefaction features were found along the river. This is not surprising given the limited exposure along the short distance traversed.

Table 4. Results of Radiocarbon Dating of Samples Collected at Study Sites.

Site - Sample No.	Lab No.	$^{13}C/^{12}C$ Ratio	^{14}C Age Yr B.P.[1]	Calibrated Age Yr B.P.[2]	Calibrated Age A.D./B.C.[2]	Sample Description
Río Culebrinas						
RC 11-C3	177892	-26.7	240 ± 40	420-390 320-270 200-150 20-0	A.D. 1530-1560 A.D. 1630-1680 A.D. 1740-1800 A.D. 1930-1950	Charred material collected 3 cm below top of dike and 2.18 m below top of cutbank
RC 13-C2	177893	-25.3	190 ± 40	300-250 230-130 110-70 30-0	A.D. 1650-1700 A.D. 1720-1820 A.D. 1840-1880 A.D. 1920-1950	Charred material collected 22 cm above sand blow
RC 13-C3	177894	-26.8	100 ± 40	280-180 150-10 0	A.D. 1670-1770 A.D. 1800-1940 A.D. 1950	Charred material collected 12 cm below sand blow and 1.74 m below top of cutbank
RC 101-C1	220013	-28.3	830 ± 40	790-680	A.D. 1160-1270	Charred material collected 20 cm below tip of dike
RC 104-C3	220016	-27.9	130 ± 40	290-0	A.D. 1660-1950	Charred material from possible tsunami deposit
RC 104-C2	220015	-23.5	130 ± 40	290-0	A.D. 1660-1950	Charred material from silty soil and 23 cm below base of possible tsunami deposit
Río Grande de Manatí						
RM 1-S2	178003	-17.5	2450 ± 40	2730-2350	780-400 B.C.	Organic sediment collected 0-3 cm above sand blow
RM 1-S1	178002	-18.3	2880 ± 40	3140-2880	1190-930 B.C.	Organic sediment collected 0-3 cm below sand blow
RM 2N-S1	197703	-18.6	1670 ± 70	1720-1410	A.D. 230-540	Organic sediment collected 3 m below surface; uppermost cm of undisturbed paleosol above graben
RM 2N-S2	197704	-15.8	3050 ± 60	3380-3017	1430-1120 B.C.	Organic sediment collected 3.4 m below surface; uppermost cm of paleosol disturbed by graben

[1] Conventional radiocarbon ages in years B.P. or before present (1950) determined by Beta Analytic, Inc. Errors represent 1 standard deviation statistics or 68% probability.

[2] Calibrated age ranges as determined by Beta Analytic, Inc., using the Pretoria procedure (Talma and Vogel, 1993; Vogel et al., 1993). Ranges represent 2 standard deviation statistics or 95% probability.

Table 4 Cont'd. Results of Radiocarbon Dating of Samples Collected at Study Sites.

Site - Sample No.	Lab No.	$^{13}C/^{12}C$ Ratio	^{14}C Age Yr B.P.[1]	Calibrated Age Yr B.P.[2]	Calibrated Age A.D./B.C.[2]	Sample Description
Río Grande de Manatí						
RM 2N-C1	197702	-25.4	4420 ± 40	5270-5170 5070-4860	3320-3220 B.C. 3120-2929 B.C.	Charred material collected 5.15 m below surface from silt in top of large sand dike
RM 4N-C2	197705	-26.8	910 ± 40	930-730	A.D. 1020-1220	Charred material collected 95 cm below sand dike tip
Río de la Plata						
RDLP 1-C1	197698	-26.9	170 ± 40	300-60 40-0	A.D. 1650-1890 A.D. 1910-1950	Charred material collected 20 cm above possible tsunami deposit
RDLP 10-C1	197699	-25.4	152.1 ± 0.6 pMC	Modern	Modern	Charred material collected from root cast through sand dike
RDLP 10-C2	197700	-25.5	1340 ± 40	1310-1180	A.D. 640-770	Charred material collected from silt 20 cm below sand dike tip
RDLP 12-C1	220010	-12.5	153.0 ± 1 pMC	270 210 140 20 0	A.D. 1680 A.D. 1740 A.D. 1800-1810 A.D. 1930 A.D. 1950	Charred material collected 30 cm above possible tsunami deposit
RDLP 12-C2	220011	-25.9	190 ± 40	300-250 230-130 110-70 30-0	A.D. 1650-1700 A.D. 1720-1820 A.D. 1840-1880 A.D. 1920-1950	Charred material collected 20 cm below possible tsunami deposit
RDLP 12-CR1	200928	-5.4	> 41000	Not applicable	Not applicable	Coral fragment
Río Espiritu Santo						
RGR 1-W1	197701	-25.3	1570 ± 60	1570-1320	A.D. 380-620	Charred material from burned log in sandy silt 6.3 m below surface
Río Blanco						
RB 1-C1	242404	-27.8	70 ± 40	270-210 140-20 0	A.D. 1680-1740 A.D. 1810-1930 A.D. 1950-1960	Wood collected about 2.7 m below top of cutbank from sandy silt

[1] Conventional radiocarbon ages in years B.P. or before present (1950) determined by Beta Analytic, Inc. Errors represent 1 standard deviation statistics or 68% probability.

[2] Calibrated age ranges as determined by Beta Analytic, Inc., using the Pretoria procedure (Talma and Vogel, 1993; Vogel et al., 1993). Ranges represent 2 standard deviation statistics or 95% probability.

Río de La Plata

We surveyed 7 km of the Río de La Plata from Highway 3 to the coast (Figure 13). Along the upstream third of the river, cutbanks were 4-5 m high and exposure was good to excellent in river bends. Interbedded reddish brown silt, in which 2-3 paleosols had developed, and cross-bedded sand overlying pebbles and cobble were exposed in the cutbanks. Along the middle third of the river, cutbanks were 2-4 m high and exposure was excellent. Cutbanks exposed reddish brown silt and interbedded silt and sand, in which up to 5 paleosols had developed. Silt and silt over sand and pebbles was detected with a soil probe up to 1.5 m below the cutbanks. Along the downstream third of the river, cutbanks were 2 m high and there was much less but good exposure in the few broad river bends. In the cutbanks, silt and interbedded silt and sand were exposed. Similar deposits were detected with a soil probe up to 1.5 m below the cutbanks.

Figure 13. Google Earth image showing portion of Río de la Plata surveyed (red line) totaling 7 km. Sand dikes were found at RDLP 10 and near RDLP 13. Site locations indicated by white dots.

Sediments along the Río de La Plata are interpreted as Holocene floodplain alluvium and include clay, silt, sand, pebbles, and cobbles (Monroe, 1963). Along the upstream third of the river, the alluvium contains more pebbles and cobbles that would reduce the liquefaction susceptibility of sediments. Evenso, a small sand dike was noted along this section. Along the middle third of the river, sedimentary conditions appear to be suitable for the formation of liquefaction features. Similar conditions likely occur downstream but the exposure is very limited. Borehole data collected at Highway 22, Dorado, and Toa Baja indicate that very loose to moderately dense sand occurs 3-9 m below the surface.

Figure 14. Sand dike crosscuts uppermost paleosol and extends 60 cm upsection. Notice that graben formed in paleosol, and presumably in overlying silt, during liquefaction event. Sample RDLP 10-2 was collected 20 cm below tip of sand dike and 40 cm above paleosol. Dating of the sample indicates that the dike formed since A.D. 640. For scale, scraper is about 32 cm long.

At site RDLP 10, we found three sand dikes, the largest being 1.5 cm wide and extending highest in the section. The largest dike crosscuts the uppermost paleosol, continues upsection for another 60 cm and pinches out about 1 m below the surface (Figure 14). The sand dike occurs along the margin of a small graben that disturbs the paleosol. The two structures probably formed during the same liquefaction event as the result of a small amount of lateral spreading. Radiocarbon dating of a sample of charred material collected 20 cm below the tip of the largest dike yielded a calibrated date of A.D. 640-770, indicating that the dike formed since A.D. 640.

The upper 65 cm of the sand dike is both iron stained and mottled. Therefore, the sand dikes probably form during the A.D. 1787 earthquake rather than the 1943 event.

At site RDLP 1 and 12, we found an unusual deposit that might be a tsunami deposit. The deposit is composed of light brown silty sand containing subangular to subrounded pieces (largest 20 cm x 15 cm x12 cm) of coral and eolianite. The deposit is 10 cm thick, about 85 cm below the top of the cutbank, and extends at least 30 m along the bank. The deposit overlies a reddish light brown paleosol developed in silty sand and is overlain by a light brown very fine sandy silt in which a 15 cm thick soil had developed. The soil horizon is overlain by a recent deposit of very fine sandy silt containing plastic. Dating of the sample RDLP 12-C2, charred material collected 20 cm below possible tsunami deposit, gave a calibrated date of A.D. 1650-1700, 1720-1820, 1840-1880, and 1920-1950, indicating that it was deposited since A.D. 1650. A sample collected 30 cm above the possible tsunami deposit gave a slightly younger age. A piece of coral from the deposit in question yielded a radiocarbon age of greater than 41 k yr, and therefore, was clearly reworked. Similar material to the possible tsunami deposit, including coral and eolianite fragments, occurs in the river-mouth bar. Perhaps this material was transported 0.75-1 km inland during a significant onshore flow. Given the results of ragdiocarbon dating and its stratigraphic position, the possible tsunami deposit probably is not related to either the 1918 or 1946 tsunamis but might be related to the 1755 Lisbon tsunami that is known to have struck other islands of the northeastern Caribbean. Also, the deposit is similar in age (A.D. 1650-1800) to an overwash deposit on Anegada, BVI that is likely due to a tsunami (Atwater et al., 2010; Reinhardt et al., 2010; Tuttle et al., 2011).

Figure 15. Unusual sandy deposit along Río de la Plata that contains pieces of coral and eolianite similar to deposit of river-mouth bar. The deposit is probably several hundred years old.

Río Canovanas

We surveyed 3.7 km of the Río Canovanas from Hwy 3 to the confluence with Río Grande de Loiza (Figure 16). We did not survey the Río Grande de Loiza because the river had been channelized and the banks were heavily vegetated.

Figure 16. Google Earth image showing portion of Río Canovanas surveyed (red line) totaling 3.7 km. Sedimentary conditions appear to be suitable for the formation of liquefaction features but none were found along this short river section. Banks of Río Grande de Loiza were heavily vegetated.

Along Río Canovanas, a tributary to Río Grande de Loiza, cutbanks were 4-6 m high and exposure was good to excellent in most river bends. Along the upstream portion of the tributary,

reddish silt was overlying interbedded silt and silty sand. Pebbley sand and pebbles were exposed at the base of the cutbank or detected with a soil probe within 0.5 m below the cutbank. Along the downstream portion of the river, reddish brown silt was overlying reddish silt in which at least one paleosol had formed. Only silt was detected with a probe up to 1.5 m below the cutbank.

Sediments along the Río Canovanas are interpreted as Holocene floodplain alluvium including silt, sand, and pebbley sand (Monroe, 1977). The sedimentary conditions appeared to be suitable for the formation of liquefaction features. No liquefaction features were found along the river but this may be due in part to the shortness of the river section that we were able to search. It is preferable to survey 10-15 km of river length to evaluate the presence or absence of liquefaction features.

Río Espiritu Santo

We surveyed 3.2 km of Río Espiritu Santo from an access point just north of Highway 3 to the police station about 1.7 km south of the coast (Figure 17). Along the upstream third of the river, cutbanks were 5-6 m high and exposure was good in river bends. Here, most of the cutbanks exposed interbedded silt and sandy silt containing paleosols. At one location, a coarse channel deposit was observed at the base of the cutbank. Elsewhere, silt and sandy silt was detected below the cutbank with a soil probe. Along the downstream two thirds of the river, the banks were heavily vegetated and there was almost no exposure. Along the lowermost 0.5 km, mangroves were growing along the banks. Where sediment was exposed or probed, we found interbedded silt and sand.

At site RGR 1, we collected sample W1 from a burned log in sandy silt at 6.3 m below surface. The sample yielded a calibrated date of A.D. 380-620 indicating that the sedimentary section along this portion of the river represents a depositional history of about 1,600 years.

Sediments along the Río Espiritu Santo are interpreted as Holocene alluvium including sand, silt, clay, and coarse channel deposits (Seiders, 1971; Pease and Briggs, 1972). We found no earthquake-induced liquefaction features along the river but this may be due to the limited amount of exposure along the river. Also, the depositional record is only about 1,600 years long and therefore, would not contain evidence of strong ground shaking prior to A.D. 380.

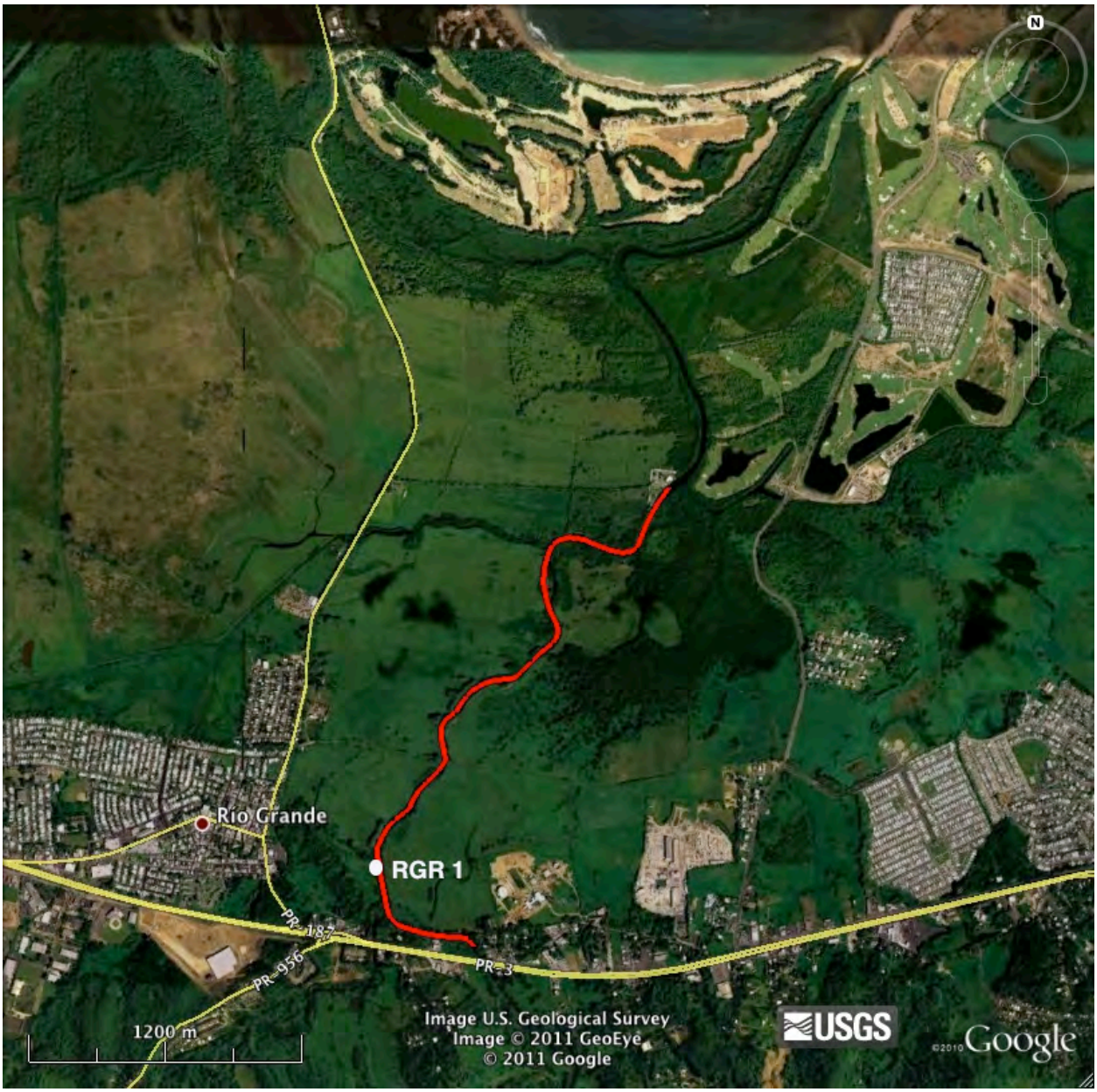

Figure 17. Google Earth image showing portion of Río Espiritu Santo surveyed (red line) totaling 3.2 km. Although sedimentary conditions may be suitable for formation of earthquake-induced liquefaction features, sediments are fairly young and exposure is limited. Wood sample from site RGR 1 was selected for dating of exposed sedimentary section.

Río Mameyes

We surveyed 4.5 km of Río Mameyes from an access point along Rt. 191 south of Highway 3 to the coast (Figure 18). Along the upstream half of the river, most cutbanks were 2-3 m high and exposure was good in river bends. Here, 1-2 m of interbedded pebbley sand and silt containing paleosols overlie a boulder-cobble deposit. Along the downstream half of the river, the banks were heavily vegetated and there was almost no exposure. Sediments along the Río Mameyes are interpreted as Holocene alluvium including sand, silt, clay, and coarse channel deposits

(Seiders, 1971; Pease and Briggs, 1972). We found no earthquake-induced liquefaction features along the Río Mameyes but this is not surprising given the coarseness (boulder and cobbles) of the deposit. Due to the high permeability of the coarse deposit, it would be difficult to buildup pore-water pressure to the point of liquefaction. Also, there was a general lack of exposure along the lower half of the river. We collected organic samples at site RMS 1 but did not select them for radiocarbon dating.

Figure 18. Google Earth image showing portion of Río Mameyes surveyed (red line) totaling 4.5 km. Sedimentary conditions do not appear to be suitable along Río Mameyes for the formation of earthquake-induced liquefaction features. We collected organic samples at site RMS 1 but did not select them for dating.

Río Fajardo

We surveyed 5.7 km of Río Fajardo from a farm road crossing of the river southeast of the airport to the sewage treatment plant about 1.6 km west of the coast (Figure 19).

Figure 19. Google Earth image showing portion of Río Fajardo surveyed (red line) totaling 5.7 km. Sedimentary conditions do not appear to be suitable along Río Fajardo for the formation of earthquake-induced liquefaction features. Site locations indicated by white dots.

Along the upstream one third of the river, most cutbanks were 7-8 m high and exposure was good to excellent in river bends. Here, 1-2 m of silt in which paleosols had developed overlies a matrix-supported pebbley cobble unit containing deformed lenses of silt and clay. In a few locations, weathered clayey silt was observed below the cobble deposit. Along the downstream two thirds of the river, cutbanks were 3-4 m high and there were fewer exposures. Here, 2-3 m

of silt containing paleosols overlies cobbles. Sediments along the Río Fajardo are interpreted as Holocene alluvial and debris avalanche deposits (Briggs and Aguilar-Cortes, 1980). We found no earthquake-induced liquefaction features along the Río Fajardo but this is not surprising given the sedimentary conditions and paucity of loose sandy sediment. We collected organic samples at site RF 2 but did not select any of them for dating.

Río Blanco

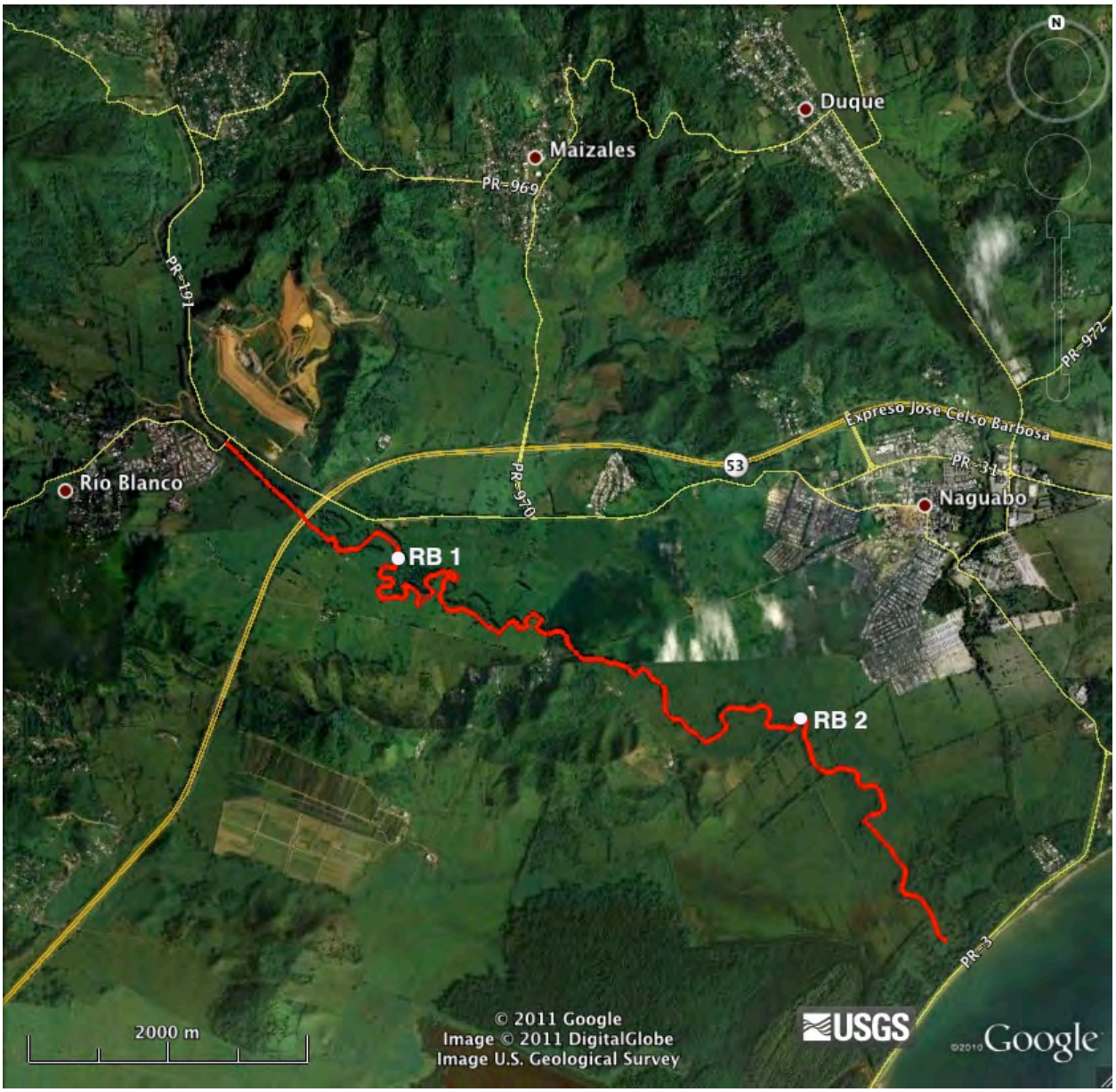

Figure 20. Google Earth image showing portion of Río Blanco surveyed (red line) totaling 10 km. Sedimentary conditions do appear to be suitable along Río Blanco for the formation of earthquake-induced liquefaction features; however, no such features were found. Site locations indicated by white dots.

We surveyed 10 km of Río Blanco from the Rt. 31 bridge in the town of Rio Blanco southeast almost to Rt. 3 along the coast (Figure 20). Along the upstream half of the river, most cutbanks were 3 m high and exposure was good to excellent in river bends (Figure 21). Typically, 1 m thick light brown silt overlies reddish silt, or interbedded silt, sandy silt, and fine to medium sand that contains one or two brown paleosols. The paleosols are characterized by blocky soil structure, manganese nodules, and root pores. Along the downstream half of the river, cutbanks were 2 m high and there were fewer exposures. As along the upper half of the river, interbedded silt and sand overlies a paleosol developed in reddish silt. Along the entire length of the river, sand and pebbley sand was observed at the base of the cutbank or detected with a soil probe below the cutbank. Sediments along the Río Blanco are interpreted as Holocene alluvium and possibly sandy beach deposits (McGonigle, 1978 and 1979). Despite careful examination of all available exposures, we found no earthquake-induced liquefaction feature along the Rio Blanco.

Figure 21. Excellent exposure of Late Holocene deposits in upstream portion of river. Note brown paleosol about 1.5 m below top of cutbank.

Unfortunately, organic samples for dating sediments along the Río Blanco were found at only one location. One of the samples, RB 1-C1, was selected for radiocarbon dating. It was a piece of wood collected 2.7 m below the top of the cutbank and 0.3 m above the water level from an organic-rich layer of gleyed sandy silt. The sample yielded calibrated dates of A.D. 1680-1740, 1810-1930, 1950-1960 (Table 4). This result indicates that the overlying fluvial sediment was deposited within the past 270 years. However, there were no paleosols exposed at this particular site suggesting that the sediment may have been younger here than elsewhere along the river. Paleosols like those observed along the Río Blanco, and described for sediments exposed along other rivers in the region such as the Río Manati and Río de la Plata, usually take several hundreds of years to form. Therefore, sedimentary sections that include paleosols elsewhere along the Río Blanco likely represent 1,000-2,000 years of depositional history.

Sedimentary conditions of silt overlying sand are suitable for the formation of earthquake-induced liquefaction features along the Río Blanco. Also, borehole data collected at the Highway 53 crossing of the river indicate that loose sand and gravelly sand susceptible to liquefaction occur between 2-5 m below the surface. Exposure along the Río Blanco is

somewhat limited especially along the lower half of the river. However, the lack of liquefaction features along the Río Blanco suggest that this area may not have been subjected to strong shaking during at least during the past 1,000-2,000 years. A paleoliquefaction study conducted for the Puerto Rico Acqeuduct and Sewage Agency found no earthquake-induced liquefaction features in Late Holocene deposits exposed in cutbanks along Rio Humacao, Rio Gurabo, Rio Loiza, and Rio Valenciano also in eastern Puerto Rico and concluded that the area had not been subjected to large earthquakes (**M** ≥ 6) produced by either the Muertos trough or the GNPRFZ during the past ~3,000 year (Tuttle and Dyer-Williams, 2006 and 2008).

Río Maunabo

Figure 22. Google Earth image showing portion of Río Maunabo surveyed (red line) totaling 4.7 km. Holocene alluvium including silt and pebbley sand were exposed in river bends but overall exposure was poor. No liquefaction features were found along this river.

We surveyed 4.7 km of Río Maunabo from a farm road crossing of the river about 2 km west of the town of Maunabo to the coast (Figure 22). Upstream cutbanks were 4-5 m high and exposure

was good to excellent in the occasional river bends. Typically, interbedded silt and sand overlies a paleosol developed in reddish clay and pebbley sandy clay. There was essentially no exposure along the lowermost 0.7 km of the river closest to the coast. These are interpreted as a Holocene alluvium overlying Pleistocene alluvium (Rogers et al., 1979). The sedimentary conditions may have been suitable for the formation of liquefaction features. Borehole data would help to assess the liquefaction susceptibility of sediments. No liquefaction features were found in any of the exposures.

Liquefaction Potential Analysis

For this project, we evaluated several scenario earthquakes to begin to place constraints on locations and magnitudes of earthquakes that induced liquefaction along the north-central coast of Puerto Rico. Using liquefaction potential analysis, we evaluated whether or not **M** 7.0 and 7.5 earthquakes at distances of 60 and 90 km and **M** 7.5 earthquakes at distances of 70, 80, 90, and 110 km would be likely, or not, to induce liquefaction along the Río Manati and the Río de la Plata. We employed the cyclic-stress method, also known as the simplified procedure (e.g., Seed and Idriss, 1982; Youd et al., 2001) and ground motion attenuation relations that seemed appropriate at the time (Boore et al., 1997; Motazedian and Atkinson, 2005). Blow counts (N, a measure of soil density) used in the analysis had been compiled previously from geotechnical reports held at the Puerto Rico Department of Transportation and Public Works.

The analysis suggests that **M** 7.5 earthquakes up to a distance of 80 km would be likely to induce liquefaction along the Rio Manati and Rio de la Plata. Similar size earthquakes at a distance of 90 km or more would be much less likely to do so. Since this analysis was performed, attenuation relations for the region have been revised. Given the sensitivity to these relations, the analysis should be repeated using the new attenuation relations before using the results to constrain the location and magnitudes of earthquakes that induced liquefaction in the region.

Conclusions

During this and earlier studies, we searched cutbanks of most major rivers along the western, northern, and eastern coasts of Puerto Rico for earthquake-induced liquefaction features. We discovered more than seventy liquefaction features along rivers in western and north-central Puerto Rico (Figure 2). Also, we found unusual deposits along the Río Culebrinas and Río Manati that might be related to 20th century tsunamis and another deposit along the Río de la Plata that is several hundred years ago and might be related to the 1755 Lisbon tsunami. Additional study of these deposits is necessary to further evaluate their origins.

In western Puerto Rico, we found at least three generations of liquefaction features along Río Culebrinas, Río Grande de Añasco, and Río Guanajibo that formed since A.D. 1300 (Tuttle et al., 2005). Many of the features formed during the 1918 earthquake of **M** 7.3 and the 1670 earthquake, which may have been as large as **M** 7 and centered in the Río Añasco valley. Liquefaction features along Río Culebrinas, and possibly a few along Río Grande de Añasco, appear to have formed in circa A.D. 1300-1508. The source area and magnitude of the A.D. A.D. 1300-1508 earthquake is, as yet, poorly understood. To induce liquefaction in northwestern Puerto Rico, however, this earthquake had to be at least **M** 6.5, even if it were a local event.

We found liquefaction features in north-central Puerto Rico along Río Grande de Manati and the Río de la Plata. We did not find liquefaction features along other rivers in northern and eastern

Puerto Rico. This may be due in part to sediments being somewhat less susceptible to liquefaction along several of the rivers, specifically Río Grande de Arecibo, Río Mameyes, and Río Fajardo. Also, the east coast is farther from many of the major earthquake sources, with the exception of the source of the A.D. 1867 earthquake in Anegada Passage. Perhaps most importantly, exposure along eastern and northeastern rivers was fairly poor due to the high rate of precipitation and heavy vegetation. In the future, another look for liquefaction features in this area would be warranted if erosion of cutbanks provides significantly improved exposure of deposits.

Along the Río Grande de Manati, we found three generations of liquefaction features that probably formed during the A.D. 1943 **M** ~7.7 and A.D. 1787 **M** ~8.0 earthquakes and an earlier event about 800 B.C. ± 400 yr. Along the Río de la Plata, small weathered sand dikes may have formed during the A.D. 1787 event. The features on the Manati that formed during the 800 B.C. event, including a 22 cm thick sand blow and 40 cm wide sand dike, are very weathered, larger than the historical features, and associated with vertical ground displacement and graben formation. The relatively large size of liquefaction features and severity of ground failures suggest that ground shaking was stronger along the north-central coast during the 800 B.C. earthquake than during the A.D. 1943 and A.D. 1787 earthquakes. This implies that the 800 B.C. earthquake was either larger than the historical earthquakes or located closer to the north-central coast of Puerto Rico. In addition, the paleoliquefaction data suggest that the earthquake source has a recurrence time of more than 2,400 years, considerably longer than that inferred for the Puerto Rico subduction zone.

A major concern in seismic hazard assessment of Puerto Rico is the importance of the eastern Septentrional fault and a possible extension of the fault east of Mona Canyon, possibly as the South Puerto Rico Slope fault (Mueller et al., 2003). The eastern Septentrional fault apparently does not offset Mona Canyon and has not produced any major earthquakes during the historic period. The 350-km length of the eastern Septentrional fault correlates with an earthquake magnitude of 8.0, and the 160-km length of the South Puerto Rico Slope fault correlates with a magnitude of 7.6. Estimates of the slip rate for the eastern Septentrional fault and the South Puerto Rico Slope fault range from 9 mm/yr to 1 mm/yr (e.g., Prentice et al, 2003b; LaForge and McCann, 2005). Four rupture scenarios derived from the slip rates are used in the 2003 USGS seismic hazard assessment for Puerto Rico. For the eastern Septentrional fault, a slip rate of 2 mm/yr implies a recurrence time of 3,600 years. For the South Puerto Rico Slope fault, a slip rate of 1 mm/yr implies a recurrence time of 3,900 years. These rates are consistent with the paleoliquefaction data gathered along the north-central coast.

One of the strands of the GNPRFZ trends towards the Río Manati valley where we found the relatively large, prehistoric liquefaction features. In the earthquake catalog used in the 2003 USGS seismic hazard assessment for Puerto Rico, two of the three shallow (depth < 50 km) onshore earthquakes of **M** ≥ 4.5 events appear to be associated with the GNPRFZ. One of these earthquakes occurred close to the Río Manati valley. The GNPRFZ is thought to be inactive and was not included as a seismic source in the seismic hazard assessment for Puerto Rico. If the GNPRFZ were found to be the source of the 800 B.C. earthquake, however, this would have significant implications for seismic hazards of the island, in general, and of San Juan and other northeastern cities, in particular.

Although significant uncertainties remain regarding the earthquake potential and recurrence rates of onshore and offshore sources, the results of this paleoliquefaction study suggest that an

earthquake in 800 B.C. ± 400 yr produced strong ground shaking along the north-central coast that exceeded that experienced during historic earthquakes. This finding indicates that there is an important seismic source in the region that could pose a significant threat to the northern coast of Puerto Rico, including the metropolitan area of San Juan.

References Cited

Asencio, E., 1980, Western Puerto Rico seismicity, U.S. Geological Survey Open-File Report 80-192, 135 p.

Atwater, B. F., U.S. ten Brink, M., Buckley, R. S. Halley, B. E. Jaffe, A. M. López-Venagas, E. G. Reinhardt, M. P. Tuttle, S. Watt, and Y. Wei, 2010, Geomorphic and stratigraphic evidence for a catastrophic tsunami or storm a few centuries ago at Anegada, British Virgin Islands, Natural Hazards, 34 p. and electronic supplement. Doi: 10.1007/s11069-010-9622-6.

Briggs, R. P., 1964, Provisional geologic map of Puerto Rico and adjacent islands, U.S. Geological Survey Miscellaneous Investigations Map I-392, scale 1:240,000.

Briggs, R. P., 1965, Geologic map of the Barceloneta quadrangle, Puerto Rico, U.S. Geological Survey, Map I-421, scale 1:20,000.

Briggs, R. P., 1968, Geologic map of the Arecibo quadrangle, Puerto Rico, U.S. Geological Survey, Map I-551, scale 1:20,000.

Briggs, R. P., and E. Aguilar-Cortes, 1980, Geologic map of the Fajardo and Icacos quadrangles, Puerto Rico, U.S. Geological Survey, Map I-1153, scale 1:20,000.

Boore, D. M., W. M. Joyner, and T. E. Fumal, 1997, Equations for estimating horizontal response spectra and peak accelerations from western North American earthquakes: A summary of recent work, Seismological Research Letters, v. 68, n. 1 p. 128-153.

Deng and Sykes, L., 1995, Determination of euler poles for Caribbean- North American plate using slip vectors of interplate earthquakes, Tectonics, v. 14, p. 39-53.

Dixon, T., F. Farina, C. DeMets, P. Jansma, P. Mann, and E. Calais, 1998, Relative motion between the Caribbean North American plates and related boundary zone deformation based on a decade of GPS observations, J. Geophys. Res., v. 103, p. 15157-15182.

Dolan, J. F., H. T. Mullins, and D. J. Wald, 1998, Active tectonics of the north-central Caribbean: Olique collision, strain partitioning, and opposing subducted slabs, in Dolan, J. F., and P. Mann, eds., Active strike-slip and collisional tectonics in the northern Caribbean plate collisional zone, Geological Society of America Special Paper 326, p. 1-61.

Geomatrix, 1988, Earthquake ground motions for the Portugues Dam, Puerto Rico, Geological-seismological evaluation to assess potential hazards, Department of the Army, Jacksonville District, Corps of Engineers, Jacksonville, Florida, 83 p., plus Appendices.

Grindlay, N. R., P. Mann, and J. Dolan, 1997, Researchers investigate submarine faults north of Puerto Rico, Eos, Trans. AGU, v. 78, p. 404.

Grindlay, N. R., M. Hearne, and P. Mann, 2005, High risk of tsunami in the northern Caribbean, EOS, Transactions, American Geophysicall Union, v. 26, n. 12, p. 121 and 126.

Jansma, P. E., G. S. Mattioli, A, Lopez, C. DeMets, T. H. Dixon, P. Mann, and E. Calais, 2000, Noetectonics of Puerto Rico and the Virgin Islands, northeastern Caribbean, from GPS geodesy, Tectonics, v. 6, p. 1021-1037.

Landers, J. F., L. S. Whiteside, and P. A. Lockridge, 2002, A brief tsunami history of tsunamis in the Caribbean Sea, The International Journal of the Tsunami Society, v. 20, n. 2, 57 p.

LaForge, R.C. and W. R. McCann, 2005, A seismic source model for Puerto Rico, for use in probabilistic ground motion hazard analyses, *in* Mann, P., ed., Active tectonics and seismic hazards of Puerto Rico, the Virgin Islands, and offshore areas: Geological Society of America Special Paper 385, p. 223-248.

Lopez, A., P. Jansma, E. Calais, C. Demets, T. Dixon, P. Mann and G. Mattioli, 1999, Microplate tectonics along the North American-Caribbean plate boundary: GPS geodetic constraints on rigidity of the Puerto Rico-Northern Virgin Islands (PRVI) block, convergence across the Muertos Trough, and extension in the Mona Canyon, Eos, Trans. AGU spring mtg suppl., S77.

Lopez, A. M., 2006, Is there a northern Lesser Antilles forearc block?, Geophysical Research Letters, v. 33. Doi: 10.1029/2005GL025293.

Mann, P., C. Schubert, and K. Burke, 1990, Review of Caribbean neotectonics. In: G. Dengo and J. E. Case (editors), The Geology of North American, v. H, The Caribbean Region. Geol. Soc. Am., Boulder, CO, p. 307-337.

Mann, P., E. Calais, J.-C. Ruegg, C. DeMets,, P.E. Jansma, and G. S. Mattioli, 2002, Oblique collision in the northeastern Caribbean from GPS measurements and geological observations, Tectonics, v. 21, n. 6. p. 1057.

Mann, P., C. Prentice, J.-C. Hippolyte, N. Grindlay, L. Abrams, and D. Lao-Davila, 2005, Reconnaissance study of Late Quaternary faulting along Cerro Goden fault zone, western Puerto Rico, in Mann, P., editor, Active tectonics and seismic hazards of Puerto Rico, the Virgin Islands and Offshore areas, Geological Society of America Special Paper 385, p. 115-138.

Masson, D. G. and K. M. Scanlon, 1991, The neotectonic setting of Puerto Rico: Geological Society of America Bulletin, v. 103, p. 144-154.

McCann, W. R., 1985, On the earthquake hazards of Puerto Rico and the Virgin Islands, Seismological Society of America Bulletin, v. 75, p. 251-262.

M'Gonigle, J., 1978, Geologic map of the Humacao quadrangle, Puerto Rico, U.S. Geological Survey, Map I-1070, scale 1:20,000.

M'Gonigle, J., 1979, Geologic map of the Naguabo and Part of the Puerca quadrangles, Puerto Rico, U.S. Geological Survey, Map I-1099, scale 1:20,000.

Monroe, W. H., 1963, Geologic map of the Vega Alta quadrangle, Puerto Rico, U.S. Geological Survey, Map I-191, scale 1:20,000.

Monroe, W. H., 1969, Geologic map of the Aguadilla quadrangle, Puerto Rico, U.S. Geological Survey, Map I-569, scale 1:20,000.

Monroe, W. H., 1971, Geologic map of the Manati quadrangle, Puerto Rico, U.S. Geological Survey, Map I-671, scale 1:20,000.

Monroe, W. H., 1977, Geologic map of the Carolina quadrangle, Puerto Rico, U.S. Geological Survey, Map I-1054, scale 1:20,000.

Monroe, W. H., 1980, Geology of the middle Tertiary formations of Puerto Rico, U.S. Geological Survey Professional Paper 953, 93 p.

Motazedian, D. and G. Atkinson, 2005, Ground-motion relations for Puerto Rico, *in* Mann, P., ed., Active tectonics and seismic hazards of Puerto Rico, the Virgin Islands, and offshore areas: Geological Society of America Special Paper 385, p. 61-80.

Moya, J.C., and W.R. McCann, 1991, Earthquake vulnerability study of Mayaguez, western Puerto Rico, Cooperative Agreement, Earthquake Safety Commission of Puerto Rico - Federal Emergency Management Agency, Internal Report 91-1: FEMAPR-0012. 66 p.

Mueller, C. S., A. D. Frankel, M. D. Petersen, and E. V. Leyendecker, 2003, Documentation for 3003 USGS seismic hazard maps of Puerto Rico and the U.S. Virgin Islands, U.S. Geological Survey, Golden, Colorado, http://eqhazmaps.usgs.gov/html/prvi2003.html.

Pease, M. H., and R. P. Briggs, 1972, Geologic map of the Rio Grande quadrangle, U.S. Geological Survey, Map I-733, scale 1:20,000.

Prentice, C. S., P. Mann, and G. Burr, 2000, Prehistoric earthquakes associated with a Late Quaternary in the Lajas Valley, Southwestern Puerto Rico, EOS Trans., American Geophysical Union, Annual Fall Meeting, p. F1182.

Prentice, C. S., H. Santos, P. Mann, M. Tuttle, E. Asencio, N. Grindlay, and J. Joyce, 2003a, Field trip: Recent tectonics and paleoseismology in western Puerto Rico, Seismological Society of America Annual Meeting, 52 p.

Prentice, C. S., P. Mann, L.R. Pena, G. Burr, 2003b, Slip rate and earthquake recurrence along the central Septentrional fault, North American-Caribbean plate boundary, Dominican Republic, Journal of Geophysical Research, v. 108, n. B3, 2149.

Prentice, C. S., and P. Mann, 2005, Paleoseismic study of the South Lajas fault: First documentation of an onshore Holocene fault in Puerto Rico, *in* Mann, P., ed., Active tectonics and seismic hazards of Puerto Rico, the Virgin Islands, and offshore areas: Geological Society of America Special Paper 385, p. 215-222.

Reid, H and S. Taber, 1919, The Puerto Rico earthquakes of October-November 1918, Bull. Seism. Soc. Amer., v. 9, p.95-127.

Reinhardt, E. G., J. Pilarczyk, and A. Brown, 2010, Probable tsunami origin for a shell and sand sheet from marine ponds on Anegada, British Virgin Islands, Natural Hazards. Doi: 10.1007/s11069-011-9730-y.

Rogers, C. L., C. M. Cram, M. H. Pease, Jr., and M. S. Tischler, 1979, Geologic map of the Yabucoa and Punta Tuna quadrangles, U.S. Geological Survey, Map I-1086, scale 1:20,000.

Seed, H. B., and I. M. Idriss, 1982, Ground motions and soil liquefaction during earthquakes, Earthquake Engineering Research Institute, Berkley, 134 p.

Seiders, V. M., 1971, Geologic map of the El Yunque quadrangle, U.S. Geological Survey, Map I-658, scale 1:20,000.

Sykes, L. R., W. R. McCann, and A. L. Kafka, 1982, Motion of Caribbean plate during last 7 million years and implications for earlier Cenozoic movements, Journal of Geophysical Research, v. 87, p. 10656-10676.

Talma, A. S., and J. C. Vogel, 1993, A simplified approach to calibrating C14 dates, Radiocarbon, v. 35, p. 317-322.

Tuttle, M. P., Prentice, C. S., Dyer-Williams, K., Pena, L. R., and Burr, G., 2003, Late Holocene liquefaction features in the Dominican Republic: A powerful tool for earthquake hazard assessment in the northeastern Caribbean, Bulletin of the Seismological Society of America, v. 93, n. 1, p. 27-46.

Tuttle, M. P., Dyer-Williams, K., Schweig, E.S., Prentice, C.S., Moya, J.C., and Tucker, K.B., 2005, Liquefaction induced by historic and prehistoric earthquakes in western Puerto Rico, *in* Mann, P., ed., Active tectonics and seismic hazards of Puerto Rico, the Virgin Islands, and offshore areas: Geological Society of America Special Paper 385, p. 263-276.

Tuttle, M. and K. Dyer-Williams, 2006, Geological evaluation studies for the Rio Valenciano dam: Liquefaction study – phase one, Technical report prepared for CSA Group, 19 pages plus 3 appendices.

Tuttle, M. and K. Dyer-Williams, 2008, Geological evaluation studies for the Rio Valenciano dam: Liquefaction study – phase two, Technical report prepared for CSA Group, 29 pages plus 1 appendix.

Tuttle, M. P., B. F. Atwater, U. S. ten Brink, R. S. Halley, and Z. Fuentes, 2011, Comparison of onshore effects of 2010 Hurricane Earl with catastrophic tsunami a few centuries ago at Anegada, British Virgin Islands, submission anticipated to Natural Hazards, *in preparation*.

Van Gestel J.-P., P. Mann, J. Dolan and N. R. Grindlay, 1998, Structure and tectonics of the upper Cenozoic Puerto Rico-Virgin Islands carbonate platform as determined from seismic reflection studies, J. Geophys. Res., v. 103, p. 30,505-30,530.

Vogel, J. C., A. Fuls, E. Visser, and B. Becker, 1993, Pretoria calibration curve for short lived samples, Radiocarbon, v. 33, p. 73-86.

Williams, P. L., and M. P. Tuttle, 2010, Seismic hazard evaluation of the Northern Puerto Rico fault zone: A case study, Seismological Society of America, Eastern Section Meeting, Program and Abstracts, p. 48.
Youd, T. L., et al., 2001, Liquefaction resistence of soils: Summary report from the 1996 NCEER and 1998 NCEER/NSF workshops on evaluation of liquefaction resistence of soils, Journal of Geotechnical and Geoenvironmental Engineering, v. 127, n. 10, p. 817-833.

Contact Information and Data Availability

Dr. Martitia P. Tuttle, Telephone: 207-371-2007, Email: mptuttle@earthlink.net.